Seasonal assembly of the phyllosphere fungal microbiome of a perennial grass is robust to nutrient addition

Running Title: Seasonal assembly of a leaf fungal microbiome

Elizabeth T. Green[1,2], Ignazio Carbone[3], Charles E. Mitchell[1]

[1] Biology Department, University of North Carolina at Chapel Hill, Chapel Hill, NC, USA

[2] School of Plant Sciences, University of Arizona, Tucson, AZ, USA

[3] Center for Integrated Fungal Research, Department of Entomology and Plant Pathology, North Carolina State University, Raleigh, NC 27695, USA

Corresponding Author:

Elizabeth Green, etgreen@arizona.edu

Abstract

The leaf microbiome plays an important role in plant health and defense. Despite its importance, how the assembly of the leaf microbial community is modified by environmental conditions such as nutrient availability remains relatively uninvestigated. Soil nutrient availability may shift the outcome of microbial interactions within a host individual or influence the pool of microbes across the plant community. We hypothesized that leaf microbial diversity would increase across the season as leaves collect additional taxa, and that this seasonal assembly would be sensitive to nutrient addition. To assess this, we tracked the assembly of the fungal phyllosphere microbiome of the grass tall fescue (*Lolium arundinaceum*) in old-field vegetation over the growing season and experimentally tested whether the seasonality of the microbiome was modified by experimental addition of soil nutrients. Fungal diversity (Shannon diversity index, richness, and evenness) increased early in the season, with most metrics saturating before the end of the season. Community composition as measured by Bray-Curtis dissimilarity also shifted over the early and mid-growing season. Phylogeny-based machine-learning identified fungal lineages that were abundant in different seasons, linking seasonal community shifts to their evolutionary context. Nutrient addition was less important than time of season, but still significantly altered community composition and interacted with time to influence richness, with lowest richness in the low nutrient addition plots early in the season. The clear seasonality of the microbiome provides support for a dynamic phyllosphere microbiome, suggesting further studies manipulating fungal recruitment over the season. Furthermore, it highlights the robustness of seasonal assembly to variation in nutrient availability.

Keywords: phenology, microbiome, phyllosphere, fungal community, community recruitment

Introduction

The leaf phyllosphere, which includes the leaf surface and interior, supports a dense and diverse community of bacteria and fungi, which interact with their hosts and each other to alter disease and herbivory [1–4] as well as nutrient cycling [5]. A leaf's microbial community is shaped by many factors including the soil microbial community, surrounding plant species, vegetation density, and seasonal environmental and abiotic fluctuations [6–10]. Despite their importance in plant health and defense, there are still large gaps in our knowledge of the structure and seasonality of the phyllosphere fungal community, including how the community assembles and varies over the season under different biotic and abiotic conditions [8, 10–13].

For most species in temperate zones, the leaf microbiome is reestablished each year and follows a successional trend. At the beginning of the growing season, many plants begin putting up new shoots and leaves. The initial, early season microbial community on those leaves is strongly related to the soil, leaf litter, and rhizosphere microbial community [13, 14]. As the season progresses, the microbial community changes in response to the environmental conditions and the influx of new microbes [12]. Later in the season, the leaf community shifts to contain more leaf-specific taxa and to mirror more closely that of surrounding plants [15].

Environmental nutrients are one of the abiotic factors that can affect the plant microbiome. Humans have increased the input of nutrients to terrestrial systems through fertilization and burning of fossil fuels [16–18], so decoding the nuanced effects of nutrients across organizational levels is imperative. Nutrient addition can alter the plant tissue nutrient concentrations and thus the resources available to microbes, which can alter the microbiome diversity and composition [19–22]. Additionally, host nutrient availability can alter the host

immune response to different microbes and the outcomes of nutrient-mediated microbial interactions [7, 23, 24]. Soil nutrients also play an important role in shaping plant communities and successional dynamics [9, 16, 25], allowing some species to flourish in environments where other species are unable to compete [26], and by altering the surrounding plant community, nutrients can indirectly alter sources of microbes for any focal plant [27–29]. Given these diverse potential effects of nutrient addition on the leaf microbiome and the seasonally dynamic assembly of leaf microbiota [8, 30], we need to understand the influence of nutrients on seasonal assembly of the leaf microbiome.

This study focused on the seasonality of the fungal community of the phyllosphere of tall fescue (*Lolium arundinaceum*). In addition to transient microbial taxa that are sporadically present throughout the season, recent research efforts have attempted to characterize the core microbial community [30–33]. The core community is a set of frequently occurring and abundant taxa that can be key players in ecosystem or organismal processes [33–36], including increasing abiotic stress tolerance, promoting growth, and protecting against foliar pathogens [8, 10, 30, 33]. The first core fungal microbiome of tall fescue was documented in 2022 [11]. We built on that study to quantify the seasonality of the core and complete fungal microbiome across the growing season and to assess the impact of soil nutrients in structuring the fungal community.

First, we hypothesized that we would see an increase in community diversity throughout the season. More specifically, we expected that early in the season a core microbial community would establish that was consistent across replicate plots, then over the season, replicate plots would diverge in community composition as different plots accumulated different microbial taxa, increasing total richness and expanding the complete community. Second, we hypothesized that soil nutrient addition would alter the phyllosphere community, perhaps by shifting within-host

81 microbial interactions, or by altering the pool of microbes across the plant community. To test
82 these two hypotheses, this study evaluated the seasonal leaf microbiome assembly in a field
83 setting and experimentally tested the influence of soil nutrients on the leaf microbiome. By
84 assessing seasonal assembly and interactions with soil nutrients, we identified a core community
85 of taxa that were the major determinants of community composition over space and time, nested
86 within the complete community that included additional taxa whose presence varied in response
87 to the season and nutrient addition.
88
89 **Methods**
90 *Field setup*
91 The experiment was conducted across a single growing season at Widener Farm (Duke
92 Forest Teaching and Research Laboratory). Widener Farm is an 8-ha old field located in Orange
93 County, North Carolina that was last cultivated in 1996 [27]. The site is dominated by perennial
94 grass and shrub species, including tall fescue (*Lolium arundinaceum*). Tall fescue supports a
95 diverse assembly of foliar, fungal pathogens that cause epidemics of several diseases over the
96 growing season, including anthracnose, brown patch, and rust [37, 38].
97 In early April of 2021, we primed and germinated tall fescue seed collected from
98 Widener Farm in 2018 by soaking seeds in water for six hours and then left them out to dry
99 overnight. We sprinkled the seed onto moist vermiculite and left them in a closed Tupperware
100 container for 10 days. After that, we haphazardly selected seedlings to transfer to individual pots
101 filled with MetroMix 360 soil. In the greenhouse, we watered the seedlings three times per week
102 for eight weeks at which point plants were hardy enough to be moved outside.

Meanwhile, we staked out 72 1m x 1m plots at Widener Farm in a 6 x12 array. On May 2, 2021, we sprayed every other plot with Roundup ® 360 and the following week covered the sprayed plots with landscaping fabric to kill all above ground vegetation. This treatment produced a checkerboard pattern of 36 sprayed and 36 unsprayed plots (Figure S1). Over three days from May 31 to June 2, 2021, we removed the landscaping fabric and transferred the seedlings from the greenhouse to the sprayed plots. We planted 12 seedlings in each plot in a 3 x 4 grid.

In a randomized blocked design with three spatial blocks of 12 plots each, we randomly assigned each plot one of three treatments of 10-10-10 N-P-K Meherrin Fertilizer (no nutrients, low nutrient addition (5 g/m^2), high nutrient addition (10 g/m^2)). This yielded four plots of each nutrient treatment in each block. In October 2021, we mowed the plots, then treated them with their assigned nutrient treatments before letting them sit undisturbed over the winter.

Sample Collection and Processing

Starting on April 29, 2022, we collected samples from the oldest leaf of three tall fescue tillers per plot, selected to be equally spaced throughout the plot, to assess the fungal microbiome of the fescue in the plots. If the oldest leaf was more than 50% chlorotic or necrotic, we collected from the second oldest leaf instead. Using an office hole punch sterilized with ethanol between samples, we collected three hole-punches of leaf tissue evenly spaced across the leaf. Hole-punches were taken of healthy tissue or tissue that was partially necrotic or diseased, but not of fully chlorotic or necrotic tissue. Leaf tissue samples were kept on ice and transported back to the University of North Carolina at Chapel Hill, about 20 minutes away, where, on the same day, we surface rinsed the samples by adding 1mL of sterile water to each sample and vortexing for 10 seconds before removing the water and freezing the samples at -80C. To retain epiphytes,

126 samples were not surface-sterilized. Samples were collected on four additional sample days
127 approximately 6 weeks apart (June 7, July 15, August 23, and October 4, 2022) for a total of 180
128 samples.

129 We ground the frozen leaf tissue samples in a ball mill (Retsch Mixer Mill) and extracted
130 DNA with the DNeasy Power Soil Pro Kit (Qiagen) following the manufacturer protocol. We
131 completed DNA amplification and library preparation and barcoding using the Quick-16S NGS
132 Library Prep Kit (Zymo Research) and substituted ITS 1-2 (ITS1: 5-
133 TCGTCGGCACGCTCACATGTGTATAAG, AGACAGCTTGGTCATTTAGAGGAAGTAA-3; ITS2: 5-
134 GTCTCGTGGGCTCGGAGATGTGTATAA, GAGACAGGCTGCGTTCTTCATCGATCS-3) primers for the
135 provided 16S primers. Library preparation was completed on two 96-well plates and five
136 samples were randomly selected as duplicate controls between plates, yielding 185 samples to
137 sequence. Samples were submitted to the High Throughput Sequencing Facility (University of
138 North Carolina at Chapel Hill) where they tested the sample quality (plate 1: 51ng/µl, 392 base
139 pairs; plate 2: 40.4 ng/µl, 373 base pairs) and sequenced the samples with a NextSeq 2000 P1
140 (Illumina) paired-end run.

141 *Data Analysis*

142 ITS sequence files were imported, demultiplexed, and denoised with the DADA2 plugin
143 [39] to Qiime2 [40]. We trimmed the primers from the reads but did not otherwise truncate reads
144 to a fixed length. Reads were merged into an amplicon sequence variant (ASV) table, and we
145 removed chimeric ASVs, also with Qiime2. The representative sequences were then
146 phylogenetically placed on a six-locus fungal reference tree [41] with the Tree-Based Alignment
147 Selector Toolkit (T-BAS v2.3) [42]. The power of phylogenetic methods largely rests on the
148 reliability of the phylogeny, which can be uninformative if based on a single locus. T-BAS
149 reduces uncertainty in the phylogenetic tree because microbiome sequences are placed on well

150 resolved multilocus reference trees. Final taxonomic assignments were based on comparing
151 placement results from T-BAS with assignments from UNITE Version 10.05.2021 [43], RDP
152 classifier Version 2.13 [44], and BLAST of ASVs against the NCBI non-redundant database
153 [45](Table S1).

154 We removed ASVs that were not assigned to the kingdom fungi and further removed
155 "nonreproducible" ASVs that were not observed at least 25 times in each of at least five samples
156 [46]. We finally removed samples with <2000 usable reads to remove outlier samples from
157 further analyses. This filtering reduced the data set to 359 ASVs and excluded 21 of the 185
158 samples. We compared the read depth of the duplicate samples to confirm limited variation
159 between the 96-well plate preparations and removed samples of each duplication at random. The
160 number of reads remaining per sample was saved to use as a representation of sampling effort in
161 further analyses. All further analyses treated ASVs as taxa. We variance normalized the count
162 data (DESeq package) [47] for ordination analyses.

163 To identify the core fungal community, we followed Shade and Stopnisek [31], an
164 approach based on each taxon's contribution to community composition, measured by Bray-
165 Curtis dissimilarity. First, to rank taxa as candidates for inclusion in the core, we calculated an
166 index for each taxon that integrated its temporal consistency and spatial occupancy. We
167 calculated the spatial occupancy of each taxon as the proportion of plots that the taxon was
168 present in, for each of the five survey dates, yielding five values of occupancy. We calculated the
169 temporal consistency of each taxon as 1 if present in all plots on a survey date or 0 if not, for
170 each of the five survey dates, yielding five values of consistency. The index value for each taxon
171 was calculated as:

172 $$Index_{taxon} = \left(\sum Spatial\ Occupancy + \sum Temporal\ Consistancy\right)/_{2}$$

Considering both occupancy and abundance allowed us to identify taxa that persisted over time through environmental disturbance events, such as rain and intense heat, as well as spatially across a population of plants. To define core membership based on contribution to variation in community composition, we calculated the mean Bray-Curtis dissimilarity for the complete data. Next, in an iterative process starting with the taxa in the first index group (i.e. the greatest index value), we calculated the mean Bray-Curtis (BC) dissimilarity for the subset and determined the proportion of community dissimilarity explained by the subset of the complete community ($1-(BC_{core}/BC_{all})$). We then proceeded in descending order to the taxa in the next lower index subset, each time adding those additional taxa to the taxa in the previous subset (Figure S2). We selected the cutoff for core taxa as where adding the next occupancy group explained a less than 0.03 difference in proportion of community dissimilarity from the complete community dissimilarity [31]. We determined the 0.03 cutoff to best describe the core community, but not the rare or transient taxa, by comparing the R^2 values of the Bray-Curtis dissimilarly analysis with the cut off at 0.01 ($R^2 = 0.498$), 0.02 ($R^2 = 0.511$), 0.03 ($R^2 = 0.528$), and 0.04 ($R^2 = 0.512$).

As metrics of alpha diversity, we calculated Shannon diversity index and taxa richness of the complete and core communities of each sample. We then calculated evenness as the Shannon diversity index divided by the natural log of richness for both communities. We used mixed-effect models with fixed effects of sampling depth (number of reads per sample), date (as a continuous variable), nutrient addition, and the date × nutrient-addition interaction (lme4 package) [48]. We nested plot within spatial block as random intercepts to account for any spatial correlations [46]. We also log transformed both metrics to reduce heteroscedasticity. We modeled each metric as a linear and quadratic function of sampling date and compared delta AIC

(linear - quadratic, positive value indicates that the quadratic model is a better fit and negative value indicates that the linear model is a better fit) values to determine which best fit the data.

To assess species composition, we conducted a Bray-Curtis dissimilarity analysis between treatments and sample dates using the variance-stabilized count data for both the complete and core communities. We ordinated the Bray-Curtis distance matrix to visualize the community relationships (vegan package) [49]. We then ran a factorial PERMANOVA (vegan, adonis2) to model the Bray-Curtis dissimilarity values against the interaction of nutrient treatment and survey date and included sampling depth as a fixed effect. The model was grouped by plot nested within block to account for spatial correlations in the sampling. We calculated the dispersion of each sample as the distance from the centroid for that survey date and nutrient treatment combination (vegan, betadispr). We then modeled the distances as a linear mixed effect model with a factorial of date and nutrient addition, with sampling depth as an additional fixed effect and plot nested within block as random intercepts.

Finally, we employed two methods to investigate whether there were specific taxa correlated with nutrient addition or survey date. First, we conducted an indicator species analysis (indicspecies package) [50] to analyze the taxa richness by the interaction of nutrient addition and survey date. Second, we applied machine learning to explore which taxa could discriminate between (A) the high vs. low nutrient treatments, and (B) the first vs. last seasonal sampling dates, using PopPhy-CNN, within T-BAS. T-BAS tracks the common ancestry of microbes because common ancestry can be both informative (e.g. in exploring correlations among traits or taxa abundances) and a source of confounding variation (e.g. in regression analysis of single and multiple traits and variables) if not dealt with in microbiome studies [51]. Moreover, phylogenetic-based methods can be essential to predictive modeling of microbiome data [52].

PopPhy-CNN applies convolutional neural networks to phylogenetic trees to identify microbial taxa that can predict system features such as an experimental treatment, location, or time [53]. To implement this approach, we first placed all ASVs on a reference tree comprising over 2,500 fungal taxa, inferred from multilocus sequence data (Fungi_v3; Accession No. 4D2ZPWQH) [41]. This reference tree was expanded from a previously published six-gene phylogeny of 214 fungal taxa [54]. As well as assigning many ASVs to taxonomic groups, this phylogenetic framework allowed us to retain both assigned and unassigned taxa for the CNN model. Phylogenetic placements were then combined with ASV count data to train the CNN models. Each model was trained using 10-fold cross validation, an L2 regularization rate of 0.001, and a kernel size of 4 (width) × 3 (height).

In our experiment, we developed two models, each of which predicted (discriminated between) two binary classes: 1) high nutrient addition with 57 samples vs. no nutrient addition (unfertilized) with 60 samples, and 2) early season (survey on 4/30/2022) with 36 samples vs. late season (survey on 10/4/2022) with 36 samples. Full taxonomic trees were pruned based on the ASVs in each dataset. For each binary class (e.g. early vs. late season), we identified taxa and lineages that discriminated between the two feature states based on feature scores derived from the first convolutional layer, which offers the highest resolution [53]. Feature scores were calculated for ASVs and for genera, then all feature scores were ranked together. Internal tree nodes with larger feature scores than their children indicate that the feature was more discriminative at a higher taxonomic level. Feature scores exceeding the 90th percentile (i.e., scores with absolute value > 1.0) were considered the most informative and examined further. Phylogenetic trees with annotated nodes and edges based on calculated feature scores were visualized using Cytoscape Version 3.10.3 [55].

Results

The final database after filtering included 359 taxa (ASVs) across 164 samples. The total number of sequence reads per sample (sampling depth) ranged from 5,802 to 448,078 with a median of 86,241 (Figure S3).

Based on the approach of Shade and Stopnisek [31], the core community comprised 54 taxa (Table S2) that were found in the first 28 ranked index values of 149 total values. These core taxa accounted for 86.6% of the total reads.

Alpha Diversity

Metrics of alpha diversity were highly structured by date for both the complete and the core community. We first tested whether the relationship of each diversity metric to time of season was better fit by linear or quadratic equations, based on AIC. Richness of the complete community increased linearly across the season (delta AIC = -38.40). Shannon diversity index, evenness, and richness of the core community were modeled best by a quadratic equation (delta AIC; complete Shannon = 18.09; core Shannon = 30.96; complete evenness = 9.55; core evenness = 20.24; core richness = 6.22). Thus, all metrics of diversity, except for richness of the complete community, increased fastest early in the season before leveling out later in the season.

For both the complete and core communities, the Shannon diversity index (complete: conditional $R^2 = 0.81$, $F_{1,164} = 127.25$, $p < 0.001$, Table S3; core: conditional $R^2 = 0.73$, $F_{1,164} = 131.21$, $p < 0.001$, Table S4; Figure 1), richness (complete: conditional $R^2 = 0.76$, $F_{1,164} = 379.92$, $p < 0.001$, Table S5; core: conditional $R^2 = 0.68$, $F_{1,164} = 107.57$, $p < 0.001$ Table S6; Figure 2), and evenness (complete: conditional $R^2 = 0.73$, $F_{1,164} = 105.83$, $p = < 0.001$, Table S7; core: conditional $R^2 = 0.70$, $F_{1,164} = 116.95$, $p < 0.001$, Table S8; Figure 3) were significantly predicted

by the survey date. Richness was also sensitive the interaction of survey date and nutrient addition for both complete and core communities with the low nutrient addition plots having the lowest taxa richness and lowest rate of richness increase across the survey dates (date * nutrients; complete: $F_{2,164} = 172.49$, $p < 0.001$, Table S5; core: $F_{2,164} = 4.74$, $p = 0.010$, Table S5).

Community Composition

When assessing the composition of the complete community, there was a clear trend across the sampling dates as the communities shifted from early to late-season and the ordination of communities moved across two axes ($F_{1,164} = 48.96$, $p < 0.001$, Table S9, Figure 4A). Survey date explained 21.3% of the variation between communities. Nutrient addition also had a significant effect but explained only 1.9% of the variation ($F_{2,164} = 2.28$, $p < 0.001$, Table S9, Figure S4A). The interaction between date and nutrient addition trended towards significant but was not significant (date * nutrients: $F_{2,164} = 1.52$, $p = 0.083$). Community dispersion (or the distance to the centroid) also increased across the season and interacted with nutrient addition (conditional $R^2 = 0.37$; date: $F_{1,164} = 68.69$, $p < 0.001$; date * nutrients: $F_{2,164} = 32.38$, $p < 0.001$ Table S10, Figure 5A).

When assessing community composition of only the core taxa, survey date explained a greater amount about of the variation, 35.2% ($F_{1,164} = 113.21$, $p < 0.001$, Table S11, Figure 4B), than when looking at the complete community. Nutrient addition explained a smaller, 0.8%, but still significant, amount of the variation ($F_{2,164} = 1.43$, $p = 0.020$, Table S10, Figure S4B), and did not interact with survey date (nutrients * survey date; $F_{2,164} = 1.40$, $p = 0.268$). Dispersion of the core community was level across the survey dates and interacted with nutrient addition with low nutrient plots decreasing in dispersion across the season while dispersion in unfertilized and high

nutrient plot remained stable (conditional $R^2 = 0.47$; date: $F_{1,164} = 10.32$, $p = 0.002$; date * nutrients: $F_{1,164} = 5.33$, $p = 0.006$, Table S12, Figure 5B).

Indicator Species Analysis

The indicator species analysis identified no taxa as significantly associated with any of the survey dates or nutrient addition treatments. The convolutional neural networks were also not able to identify fungal lineages that predicted nutrient addition treatment (unfertilized feature score = 0.95, high nutrient addition feature score = -0.49), but the neural networks did identify fungal lineages that predicted survey date (early season feature score = 1.69, late season feature score = -1.70). There were 15 highly predictive taxa for early season communities and 22 highly predictive taxa of late season communities (Table S13; Figure S5). *Cladosporium* accounted for the top three predictive lineages and the top predictive taxon (ASV 40) for early season communities, while *Leucosporidium* had the greatest number of lineages (5) predictive for early season communities (Table S13). In late season communities, *Bulleribasidium* had the greatest number of predictive lineages (4) and the most predictive taxon (ASV 57).

Discussion

There was a clear increase in community diversity across the seasonal surveys, in support of our first hypothesis. All three metrics of alpha diversity (Shannon diversity index, species richness, and species evenness) displayed increasing diversity early in the season for both the complete and the core microbiomes. Shannon diversity and evenness increased quadratically for both sets of communities with the fastest increase occurring early in the season before leveling off. Species richness increased quadratically for the core community, but richness of the complete community increased linearly across the season, suggesting that the complete and core

309 microbiomes added taxa at different rates throughout the season. We identified a core
310 community of 54 taxa. The remaining 305 taxa were transient and together contributed only 3%
311 to the dissimilarity of the complete community [31]. This core community suggests that there is a
312 consistent collection of fungi in the phyllosphere of tall fescue that comprises of a dominant set
313 of taxa throughout the season, lending support to our hypothesis that the core complete
314 communities add taxa at different rates.

315 One way to interpret the difference in richness trajectory between the complete and core
316 communities is through the lens of community succession of the phyllosphere [8, 12, 30, 56].
317 Early in the spring, tall fescue plants begin to put up new tillers and collect microbes from the
318 soil and surrounding environment. Some fungi may overwinter in the root tissue and be
319 vertically transmitted to the new tillers or in the soil but given the low species richness early in
320 the season, this seems to be the minority of taxa [14, 57]. The new tillers begin recruiting
321 microbes and soon have collected their community of core taxa. Throughout the rest of the
322 season, more transient fungi continue to colonize the leaves and the phyllosphere shifts from a
323 lower diversity, more homogenous early-successional community to a diverse and varied late-
324 successional community. Once the core taxa became established, it persisted for the remainder of
325 the season resulting in quadratic growth [8, 56]. However, the complete community recruited
326 taxa at a consistent rate throughout the season resulting in linear growth.

327 The complete community was also much more variable over time, which included
328 recruiting and losing taxa between survey dates. These stochastically present species are known
329 as conditionally rare taxa and have been found to disproportionately contribute to temporal
330 changes in the microbiome [58, 59]. While we did not identify indicator species between the
331 survey dates, there were distinct fungal lineages associated with early and late season

communities in the phylogenetic neural networks, suggesting that, for some taxa, shared evolutionary history can help predict their role in seasonal assembly of the microbiome. *Cladosporidium* was highly predictive of early season communities and *Bulleribasidium* was most predictive of late season communities. Both taxa were identified within the core community, suggesting that they are persistently present but shifting in prevalence across the season. *Cladosporium* is an abundant genus in the soil and plant tissue that has been identified as both an endophyte [60] and plant pathogen [61] of tall fescue. Additional research has found *Bulleribasidium* to be a parasite of *Cladosporium* [62] suggesting parasitism could be the mechanism for the decline in *Cladosporium* and the rise in *Bulleribasidium* from the start to the end of the season.

Community composition further supports our first hypothesis as there was a clear shift in Bray-Curtis dissimilarity of the communities from early- to late-season samples. The dispersion of samples as measured by their distance from the centroid NMDS values of each survey date increased across the season for the complete community and decreased for the core community. Despite adding new taxa and leaf communities diverging from each other, tall fescue maintained its core community throughout the season. Combining our understanding of core and conditionally rare taxa could help us to identify the mechanisms leading recruitment and loss of taxa in the phyllosphere as plants grow throughout a season.

We also found support for our second hypothesis that soil nutrients would influence the fungal community. Taxa richness of both the complete and core communities was significantly affected by nutrients and the interaction between nutrients and survey date. Richness of the low nutrient plots increased more slowly than richness of either the unfertilized or high nutrient plots, suggesting a non-linear effect of nutrients on the phyllosphere. Dispersion of the communities

355 from the centroid was also influenced by nutrient addition with composition of the unfertilized
356 plots experiencing increased dispersion compared to the low and high nutrient plots. Since these
357 trends were observed for both the complete and core communities, it does not support
358 conditionally rare species being responsible for the interaction with nutrients and instead
359 suggests that both common and rare species of fungi are responding to soil nutrients. We found a
360 significant effect of nutrients on community composition and a trend towards, but not significant
361 interaction, between nutrients and date for the complete community.

362 Previous studies have found an consistent effect of nutrients on the soil and phyllosphere
363 community at the site level [6, 25]. Our findings support this conclusion but also advise a more
364 nuanced approach to future studies, since the response to nutrient addition was nonlinear and not
365 consistent. Community richness increased with low nutrient addition and community dispersion
366 decreased with low and high nutrient addition. We applied a complete nutrient N-P-K fertilizer
367 and thus cannot separate the effect of individual nutrients on the fungal community [63].
368 Additionally, due to the nonlinear effect of nutrients, it is important to pursue further research
369 into the effect of a finer gradient of nutrient addition on the phyllosphere community to identify
370 the tipping points where nutrient addition decreases richness and where richness begins to
371 increase again.

372 When assessed in relationship to each other these results help to address the nexus of
373 effects that seasonality and soil nutrients have on the phyllosphere microbiome. We found strong
374 support for our first hypothesis that fungal diversity would increase early in the season as leaves
375 recruit more taxa and identified the difference in the temporal variation of taxa richness between
376 the complete and core communities. We also found modest support for our second hypothesis
377 that soil nutrients would play a role in shaping the phyllosphere community. Further research

into this seasonality could help us to better understand succession of fungal communities and how the microbiome reacts to and protects against seasonal epidemics of foliar pathogens [10, 12]. Investigating the role that each of the core taxa play within the microbiome community could illuminate mechanisms by which the core taxa influence functioning of the leaf, in the context of biotic and abiotic stress [30, 32, 33].

Acknowledgements

This work was supported by the NSF-USDA joint program in Ecology and Evolution of Infectious Diseases (USDA-NIFA AFRI grant no. 2016-67013-25762 and NSF grant DEB-2308472). We would like to thank E. Snyder and B. Stiver for help with sample collection, and J. White for integrating PopPhy-CNN into T-BAS.

References

1. Berg M, Koskella B. Nutrient- and Dose-Dependent Microbiome-Mediated Protection against a Plant Pathogen. *Curr Biol* 2018;**28**:2487-2492.e3. https://doi.org/10.1016/j.cub.2018.05.085
2. Busby PE, Peay KG, Newcombe G. Common foliar fungi of Populus trichocarpa modify Melampsora rust disease severity. *New Phytol* 2016;**209**:1681–1692. https://doi.org/10.1111/nph.13742
3. Humphrey PT et al. Diversity and abundance of phyllosphere bacteria are linked to insect herbivory. *Mol Ecol* 2014;**23**:1497–1515. https://doi.org/10.1111/mec.12657
4. Ritpitakphong U et al. The microbiome of the leaf surface of Arabidopsis protects against a fungal pathogen. *New Phytol* 2016;**210**:1033–1043. https://doi.org/10.1111/nph.13808

5. Fürnkranz M et al. Nitrogen fixation by phyllosphere bacteria associated with higher plants and their colonizing epiphytes of a tropical lowland rainforest of Costa Rica. *ISME J* 2008;**2**:561–570. https://doi.org/10.1038/ismej.2008.14
6. Seabloom EW et al. Globally consistent response of plant microbiome diversity across hosts and continents to soil nutrients and herbivores. *Nat Commun* 2023;**14**:3516. https://doi.org/10.1038/s41467-023-39179-w
7. Borer ET et al. The world within: Quantifying the determinants and outcomes of a host's microbiome. *Basic Appl Ecol* 2013;**14**:533–539. https://doi.org/10.1016/j.baae.2013.08.009
8. Grady KL et al. Assembly and seasonality of core phyllosphere microbiota on perennial biofuel crops. *Nat Commun* 2019;**10**:4135. https://doi.org/10.1038/s41467-019-11974-4
9. Liu X et al. Species decline under nitrogen fertilization increases community-level competence of fungal diseases. *Proc R Soc B Biol Sci* 2017;**284**:20162621. https://doi.org/10.1098/rspb.2016.2621
10. Trivedi P et al. Plant–microbiome interactions: from community assembly to plant health. *Nat Rev Microbiol* 2020;**18**:607–621. https://doi.org/10.1038/s41579-020-0412-1
11. Dale JCM, Newman JA. A First Draft of the Core Fungal Microbiome of Schedonorus arundinaceus with and without Its Fungal Mutualist Epichloë coenophiala. *J Fungi* 2022;**8**:1026. https://doi.org/10.3390/jof8101026
12. Debray R et al. Priority effects in microbiome assembly. *Nat Rev Microbiol* 2022;**20**:109–121. https://doi.org/10.1038/s41579-021-00604-w
13. Gao C et al. Fungal community assembly in drought-stressed sorghum shows stochasticity, selection, and universal ecological dynamics. *Nat Commun* 2020;**11**:34. https://doi.org/10.1038/s41467-019-13913-9

14. Kong HG, Song GC, Ryu C-M. Inheritance of seed and rhizosphere microbial communities through plant–soil feedback and soil memory. *Environ Microbiol Rep* 2019;**11**:479–486. https://doi.org/10.1111/1758-2229.12760

15. Gao F-L et al. Cascading effects of nitrogen, rhizobia and parasitism via a host plant. *Flora* 2019;**251**:62–67. https://doi.org/10.1016/j.flora.2018.12.007

16. Keller AB et al. Stronger fertilization effects on aboveground versus belowground plant properties across nine U.S. grasslands. *Ecology* 2023;**104**:e3891. https://doi.org/10.1002/ecy.3891

17. Steffen W et al. Planetary boundaries: Guiding human development on a changing planet. 2015;**347**:736. https://doi.org/10.1126/science.1259855

18. Veresoglou SD et al. Fertilization affects severity of disease caused by fungal plant pathogens. *Plant Pathol* 2013;**62**:961–969. https://doi.org/10.1111/ppa.12014

19. Lumibao CY et al. Site-specific responses of foliar fungal microbiomes to nutrient addition and herbivory at different spatial scales. *Ecol Evol* 2019;**9**:12231–12244. https://doi.org/10.1002/ece3.5711

20. Firn J et al. Leaf nutrients, not specific leaf area, are consistent indicators of elevated nutrient inputs. *Nat Ecol Evol* 2019;**3**:400–406. https://doi.org/10.1038/s41559-018-0790-1

21. Tellez PH et al. Traits along the leaf economics spectrum are associated with communities of foliar endophytic symbionts. *Front Microbiol* 2022;**13**.

22. Oono R et al. Species diversity of fungal endophytes across a stress gradient for plants. *New Phytol* 2020;**228**:210–225. https://doi.org/10.1111/nph.16709

445 23. Lacroix C, Seabloom EW, Borer ET. Environmental nutrient supply alters prevalence and
446 weakens competitive interactions among coinfecting viruses. *New Phytol* 2014;**204**:424–
447 433. https://doi.org/10.1111/nph.12909
448 24. Smith KF, Acevedo-Whitehouse K, Pedersen AB. The role of infectious diseases in
449 biological conservation. *Anim Conserv* 2009;**12**:1–12. https://doi.org/10.1111/j.1469-
450 1795.2008.00228.x
451 25. Ramirez KS, Craine JM, Fierer N. Consistent effects of nitrogen amendments on soil
452 microbial communities and processes across biomes. *Glob Change Biol* 2012;**18**:1918–
453 1927. https://doi.org/10.1111/j.1365-2486.2012.02639.x
454 26. Arnillas CA et al. Opposing community assembly patterns for dominant and nondominant
455 plant species in herbaceous ecosystems globally. *Ecol Evol* 2021;**11**:17744–17761.
456 https://doi.org/10.1002/ece3.8266
457 27. Heckman RW, Wright JP, Mitchell CE. Joint effects of nutrient addition and enemy
458 exclusion on exotic plant success. *Ecology* 2016;**97**:3337–3345.
459 https://doi.org/10.1002/ecy.1585
460 28. Heckman RW, Halliday FW, Mitchell CE. A growth–defense trade-off is general across
461 native and exotic grasses. *Oecologia* 2019;**191**:609–620. https://doi.org/10.1007/s00442-
462 019-04507-9
463 29. Mitchell CE, Tilman D, Groth JV. Effects of Grassland Plant Species Diversity, Abundance,
464 and Composition on Foliar Fungal Disease. *Ecology* 2002;**83**:1713–1726.
465 https://doi.org/10.1890/0012-9658(2002)083[1713:EOGPSD]2.0.CO;2
466 30. Howe A et al. Seasonal activities of the phyllosphere microbiome of perennial crops. *Nat*
467 *Commun* 2023;**14**:1039. https://doi.org/10.1038/s41467-023-36515-y

31. Shade A, Stopnisek N. Abundance-occupancy distributions to prioritize plant core microbiome membership. *Curr Opin Microbiol* 2019;**49**:50–58. https://doi.org/10.1016/j.mib.2019.09.008

32. Custer GF et al. Comparative Analysis of Core Microbiome Assignments: Implications for Ecological Synthesis. *mSystems* 2023;**8**:e01066-22. https://doi.org/10.1128/msystems.01066-22

33. Shade A, Handelsman J. Beyond the Venn diagram: the hunt for a core microbiome. *Environ Microbiol* 2012;**14**:4–12. https://doi.org/10.1111/j.1462-2920.2011.02585.x

34. Hernandez-Agreda A, Gates RD, Ainsworth TD. Defining the Core Microbiome in Corals' Microbial Soup. *Trends Microbiol* 2017;**25**:125–140. https://doi.org/10.1016/j.tim.2016.11.003

35. Umaña MN et al. A core-transient framework for trait-based community ecology: an example from a tropical tree seedling community. *Ecol Lett* 2017;**20**:619–628. https://doi.org/10.1111/ele.12760

36. Cantoran A et al. Defining a core microbial necrobiome associated with decomposing fungal necromass. *FEMS Microbiol Ecol* 2023;**99**:fiad098. https://doi.org/10.1093/femsec/fiad098

37. Halliday FW et al. Past is prologue: host community assembly and the risk of infectious disease over time. *Ecol Lett* 2019;**22**:138–148. https://doi.org/10.1111/ele.13176

38. Grunberg RL et al. Disease decreases variation in host community structure in an old-field grassland. *PLOS ONE* 2023;**18**:e0293495. https://doi.org/10.1371/journal.pone.0293495

39. Callahan BJ et al. DADA2: High-resolution sample inference from Illumina amplicon data. *Nat Methods* 2016;**13**:581–583. https://doi.org/10.1038/nmeth.3869

40. Bolyen E et al. Reproducible, interactive, scalable and extensible microbiome data science using QIIME 2. *Nat Biotechnol* 2019;**37**:852–857. https://doi.org/10.1038/s41587-019-0209-9

41. Carbone I, White JB. T-BAS v2.4: Phylogenetic-data repository and tool for phylogeny-based placement. 2025. https://doi.org/10.52750/634503

42. Carbone I et al. T-BAS Version 2.1: Tree-Based Alignment Selector Toolkit for Evolutionary Placement of DNA Sequences and Viewing Alignments and Specimen Metadata on Curated and Custom Trees. *Microbiol Resour Announc* 2019;**8**:e00328-19. https://doi.org/10.1128/MRA.00328-19

43. Põlme S et al. FungalTraits: a user-friendly traits database of fungi and fungus-like stramenopiles. *Fungal Divers* 2020;**105**:1–16. https://doi.org/10.1007/s13225-020-00466-2

44. Wang Q, Cole JR. Updated RDP taxonomy and RDP Classifier for more accurate taxonomic classification. *Microbiol Resour Announc* 2024;**13**:e01063-23. https://doi.org/10.1128/mra.01063-23

45. Camacho C et al. BLAST+: architecture and applications. *BMC Bioinformatics* 2009;**10**:421. https://doi.org/10.1186/1471-2105-10-421

46. Wagner MR, Busby PE, Balint-Kurti P. Analysis of leaf microbiome composition of near-isogenic maize lines differing in broad-spectrum disease resistance. *New Phytol* 2020;**225**:2152–2165. https://doi.org/10.1111/nph.16284

47. Love MI, Huber W, Anders S. Moderated estimation of fold change and dispersion for RNA-seq data with DESeq2. *Genome Biol* 2014;**15**:550. https://doi.org/10.1186/s13059-014-0550-8

512 48. Bates D et al. Fitting Linear Mixed-Effects Models Using lme4. *J Stat Softw* 2015;**67**:1–48.
513 https://doi.org/10.18637/jss.v067.i01
514 49. Oksanen J et al. vegan: Community Ecology Package. 2022. 2022.
515 50. Cáceres MD, Legendre P. Associations between species and groups of sites: indices and
516 statistical inference. *Ecology* 2009;**90**:3566–3574. https://doi.org/10.1890/08-1823.1
517 51. Washburne AD et al. Methods for phylogenetic analysis of microbiome data. *Nat Microbiol*
518 2018;**3**:652–661. https://doi.org/10.1038/s41564-018-0156-0
519 52. Xiao J et al. Predictive Modeling of Microbiome Data Using a Phylogeny-Regularized
520 Generalized Linear Mixed Model. *Front Microbiol* 2018;**9**:1391.
521 https://doi.org/10.3389/fmicb.2018.01391
522 53. Reiman D et al. PopPhy-CNN: A Phylogenetic Tree Embedded Architecture for
523 Convolutional Neural Networks to Predict Host Phenotype From Metagenomic Data. *IEEE*
524 *J Biomed Health Inform* 2020;**24**:2993–3001. https://doi.org/10.1109/JBHI.2020.2993761
525 54. James TY et al. Reconstructing the early evolution of Fungi using a six-gene phylogeny.
526 *Nature* 2006;**443**:818–822. https://doi.org/10.1038/nature05110
527 55. Shannon P et al. Cytoscape: a software environment for integrated models of biomolecular
528 interaction networks. *Genome Res* 2003;**13**:2498–2504. https://doi.org/10.1101/gr.1239303
529 56. Copeland JK et al. Seasonal Community Succession of the Phyllosphere Microbiome. *Mol*
530 *Plant-Microbe Interactions*® 2015;**28**:274–285. https://doi.org/10.1094/MPMI-10-14-
531 0331-FI
532 57. Otten W et al. Soil physics, fungal epidemiology and the spread of *Rhizoctonia solani*. *New*
533 *Phytol* 2001;**151**:459–468. https://doi.org/10.1046/j.0028-646x.2001.00190.x

534 58. Shade A et al. Conditionally Rare Taxa Disproportionately Contribute to Temporal Changes
535 in Microbial Diversity. *mBio* 2014;**5**:10.1128/mbio.01371-14.
536 https://doi.org/10.1128/mbio.01371-14
537 59. Zuo Y et al. The importance of conditionally rare taxa for the assembly and interaction of
538 fungal communities in mangrove sediments. *Appl Microbiol Biotechnol* 2022;**106**:3787–
539 3798. https://doi.org/10.1007/s00253-022-11949-4
540 60. Clarke BB et al. Endophyte-Mediated Suppression of Dollar Spot Disease in Fine Fescues.
541 *Plant Dis* 2006;**90**:994–998. https://doi.org/10.1094/PD-90-0994
542 61. Varga Z, Fischl G. Fungal infection of cultivated grass seeds. *Cereal Res Commun*
543 2006;**34**:1291–1297. https://doi.org/10.1556/CRC.34.2006.4.271
544 62. Sampaio JP et al. New taxa in the Tremellales: Bulleribasidium oberjochense gen. et sp.
545 nov., Papiliotrema bandonii ge. *Mycologia* 2002;**94**:873–887.
546 63. Dordas C. Role of nutrients in controlling plant diseases in sustainable agriculture. A review.
547 *Agron Sustain Dev* 2008;**28**:33–46.
548

549 **Data Accessibility**

550 Raw sequence reads, processed data, code, and related metadata are available on DataDryad
551 (https://doi.org/10.5061/dryad.02v6wwqfd).
552 Benefits Generated: Benefits from this research accrue from the sharing of our data and results
553 on public databases as described above.
554

555 **Author Contributions:**

556 E.T.G and C.E.M. conceived ideas and designed methodology; E.T.G. performed field

557 collections and laboratory work; E.T.G. performed analyses and led writing of the manuscript.

558 I.C. performed additional analyses. All authors contributed critically to drafts and gave final

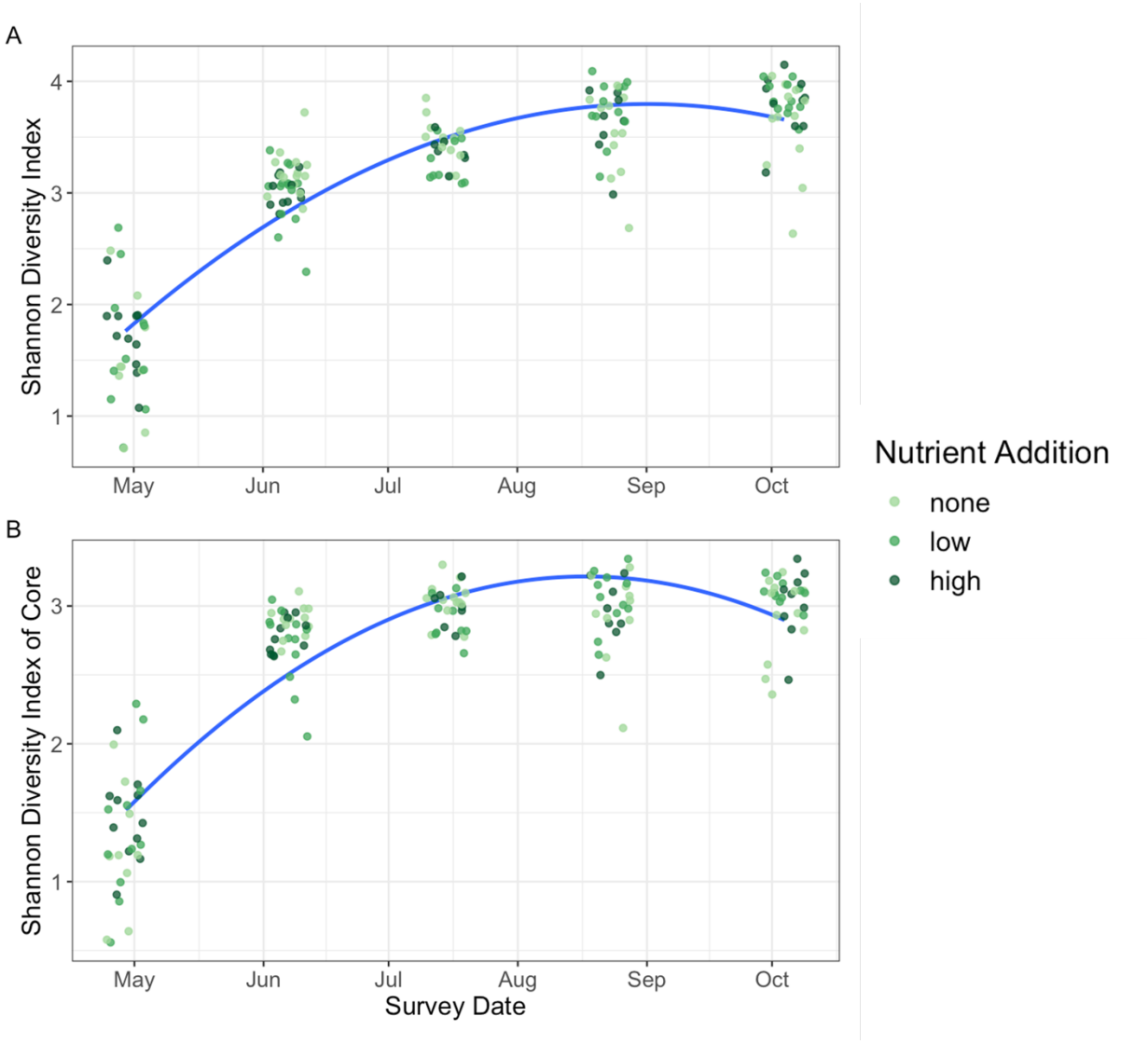

559

560 **Figure 1.** Shannon diversity index of complete (A) and core (B) communities across survey

561 dates with quadratic fit lines. For both, diversity increased early in the season, then leveled off.

562 Colors represent the nutrient addition treatment.

563

564

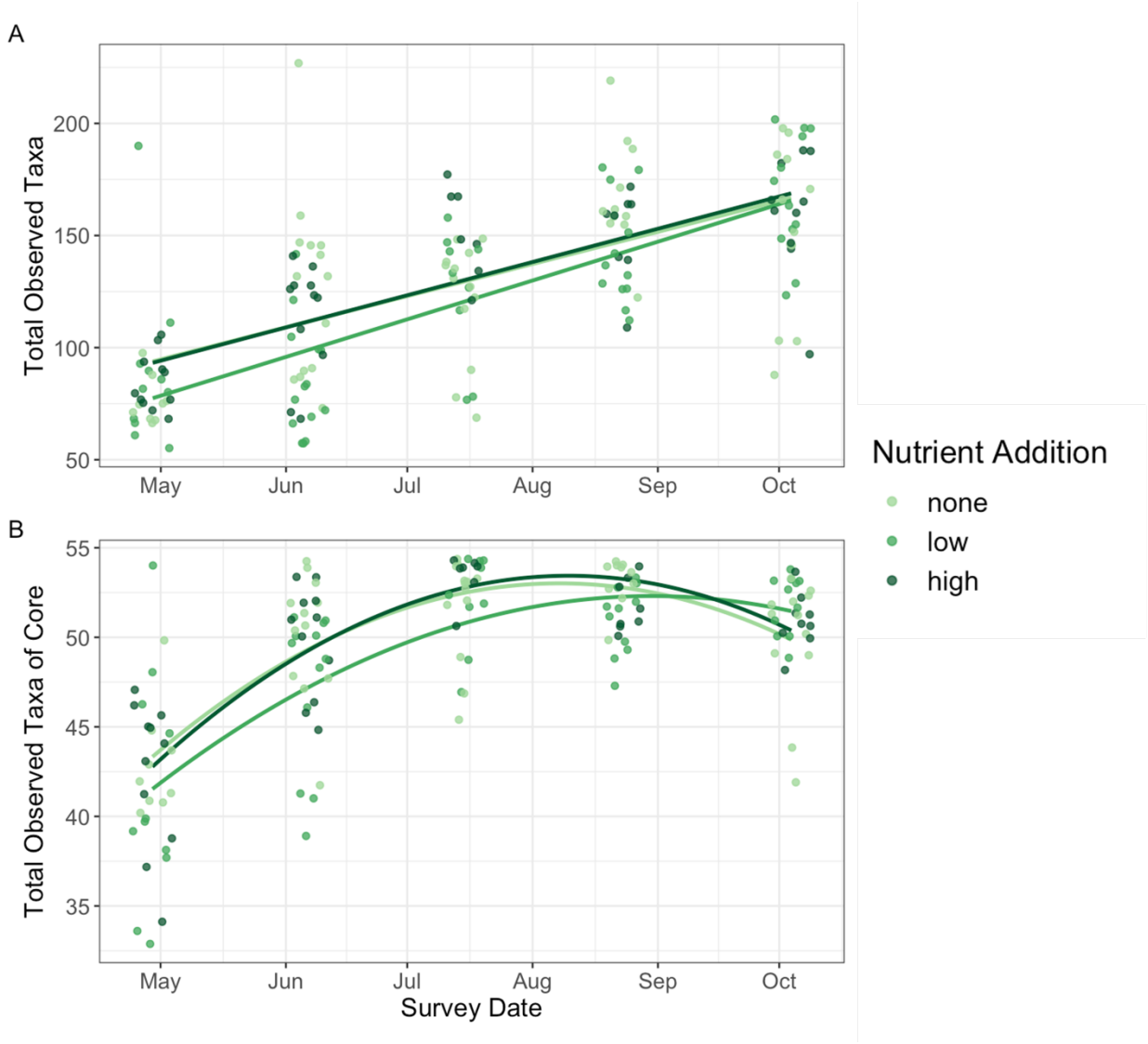

Figure 2. Taxa richness across survey dates for the complete (A, linear) and core (B, quadratic) communities. For both, there was a statistically significant interaction between nutrient addition and survey date, with the lowest taxa richness in the low nutrient addition plots early in the season. Color represents the nutrient addition treatment.

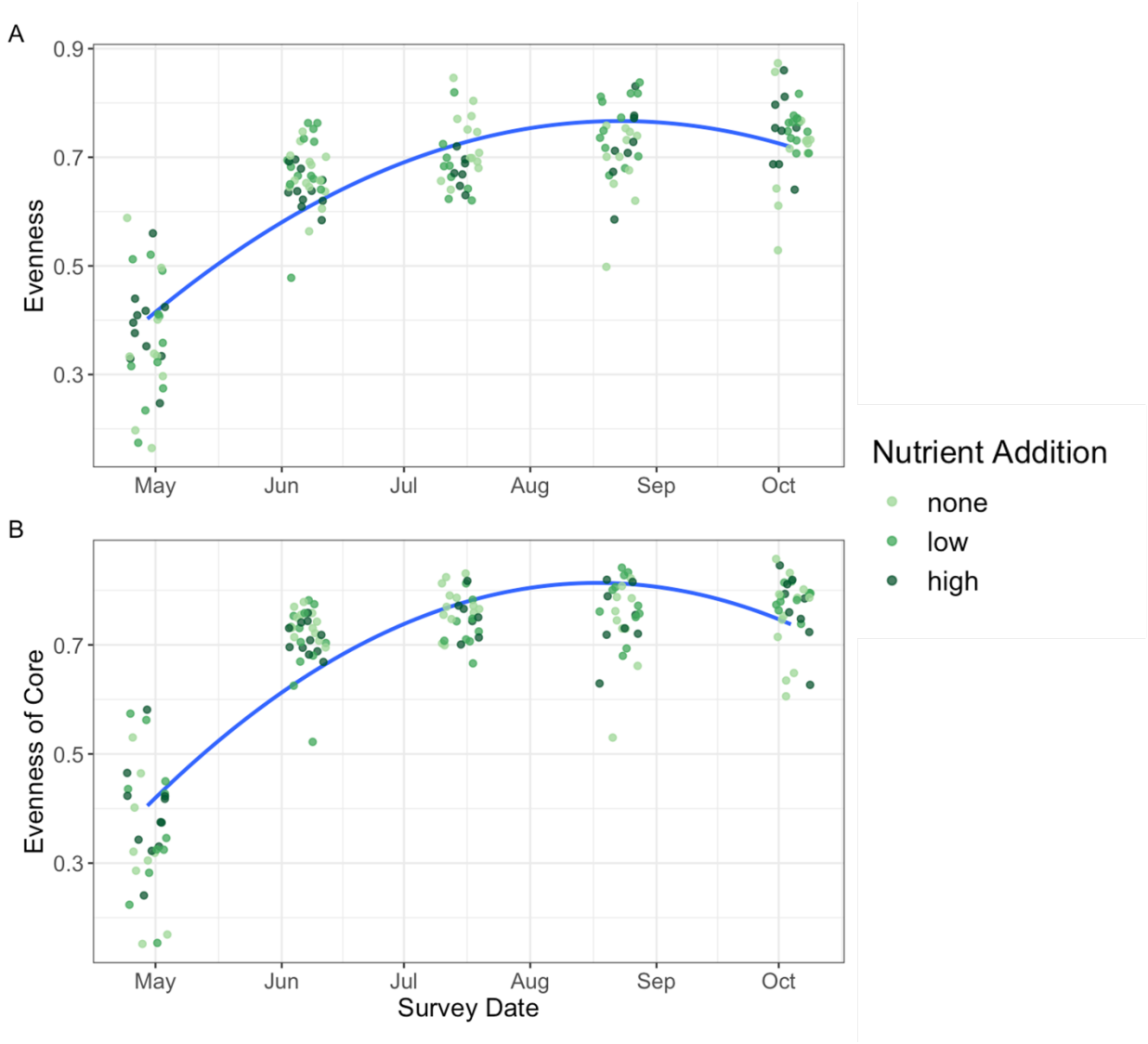

570

571 **Figure 3.** Taxa evenness across survey dates for the complete (A) and core (B) community with

572 quadratic fit lines. For both, evenness increased early in the season, then leveled off. Color

573 represents the nutrient addition treatment.

574

575

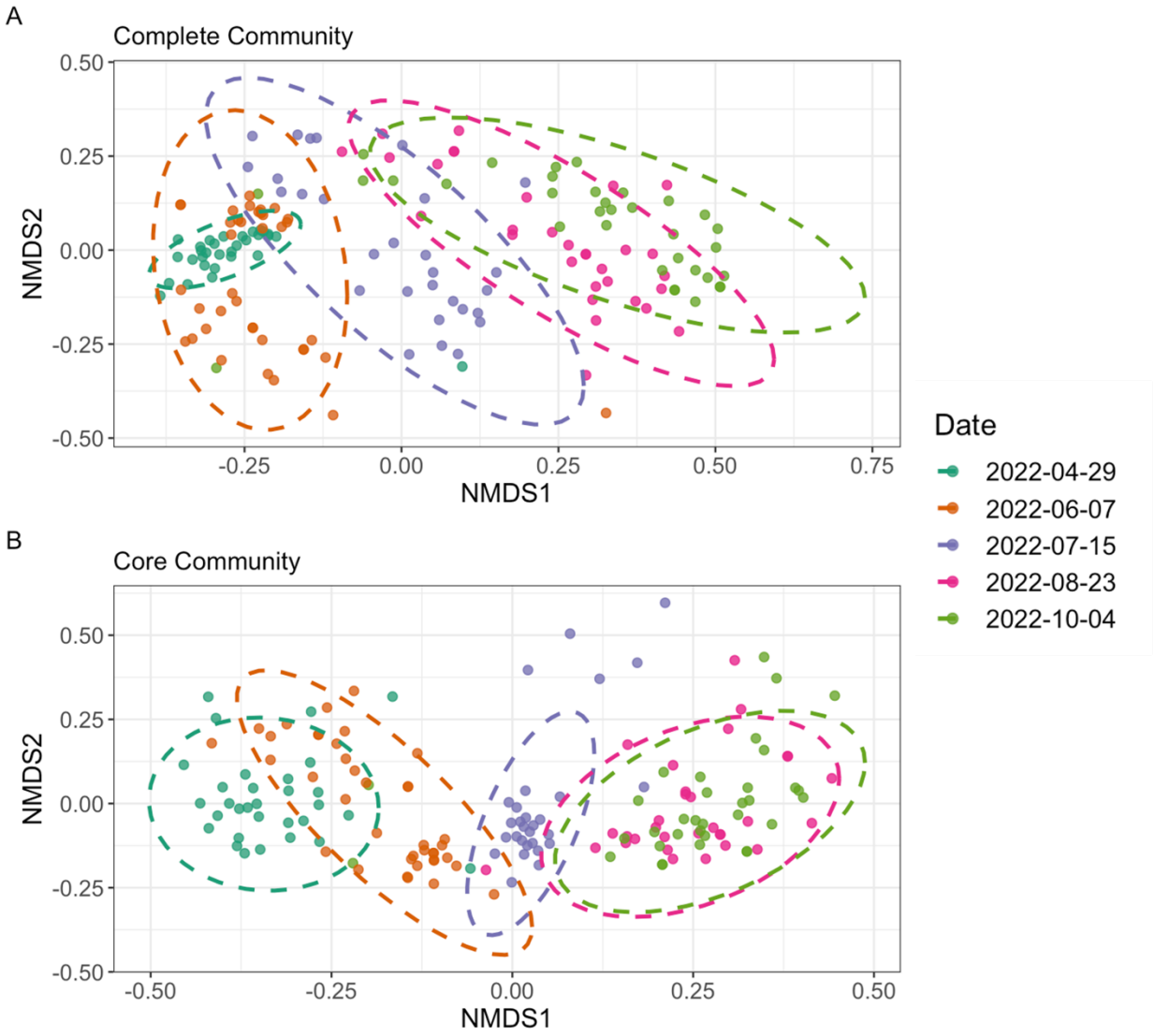

576

577 **Figure 4.** NMDS based on Bray-Curtis dissimilarity of the complete (A) and core (B) fungal

578 taxa in each plot, grouped by survey date. 95% confidence ellipses are shown for each date.

579

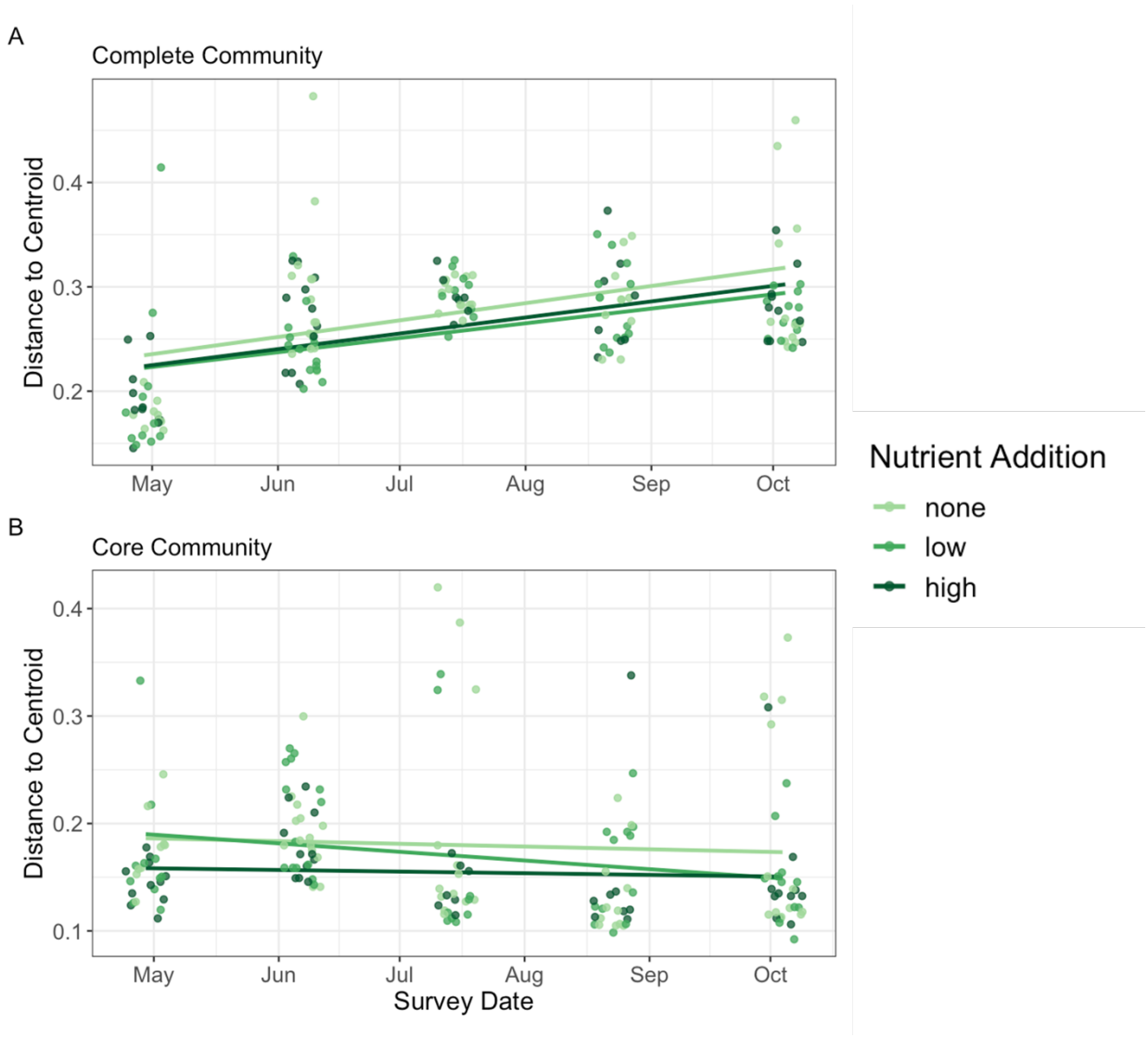

580

581 **Figure 5.** Community dispersion as measured by the distance to centroid of each survey date for

582 the NMDS based on the Bray-Curtis dissimilarity of the complete (A) and core (B) fungal taxa in

583 each plot. Color represents the nutrient treatment.